Morphology and lateral distribution of self-organized InP islands grown on $Ga_xIn_{1-x}P$ buffer layers

Songhao Liu (刘颂豪)[1], Hao Wang (王 浩)[1], Gucheng Zeng (曾谷城)[2],
Yangzhe Wu (吴扬哲)[2], Jiye Cai (蔡继业)[2], Guanghan Fan (范广涵)[1], and Changjun Liao (廖常俊)[1]

[1]*School for Information and Optoelectronic Science and Engineering,*
South China Normal University, Guangzhou 510631
[2]*Department of Chemistry, Jinan University, Guangzhou 510632*

The morphology of self-organized InP islands on GaInP buffer layers were probed by the whole island energy and surface energy. The island morphology was affected by Mismatch between $Ga_xIn_{1-x}P$ buffer layer and InP island (MBI). With MBI increasing, the island elongates itself. The calculation also shows that the island metamorphosis was elongated with the increasing of the island volume. The morphology of different $InP/Ga_xIn_{1-x}P$ systems, grown on GaAs substrate by metal organic chemical vapor deposition (MOCVD) method, was consistent with calculations. The self-organized islands at the surface of buffer layers were analyzed by scaling theories to show a periodical distribution. Buffer layers such as the mismatched GaInP on the GaAs (100) tilt to (111) 15° could improve the periodicity of the island separation distribution. The result also shows that the dislocations had different functions in island distribution along different directions, [110] and [1-10] directions.

OCIS codes: 160.0160, 180.0180, 000.2190.

Semiconductor nanostructure including quantum dots and quantum wires is of great interest due to their unique optoelectronic properties for fundamental research and practical application[1−9]. It is well known that there are varies typical shapes of self-organized islands including pyramid, circle, cone, hut, triangle, etc.[8−14]. To explain the evolution of the morphology of self-organized islands, thermodynamic, kinetics, and Monte-Carlo model have been introduced[4−7], and the system of Si_xGe_{1-x}/Si, $Ga_xIn_{1-x}As/InP$, $Ga_xIn_{1-x}As/GaAs$, InP/GaInP have been studied carefully[8−16]. Current researches showed that there are many parameters and mechanisms that influence self-organized island shape, for instance, surface energy, growth method, buffer layer, growth temperature, growth speed, and annealing, etc.[12−16]. The island elongation is especially useful for the growth of nanowires and should affect the optoelectronic properties significantly[1,2]. Therefore the elongation and the mechanism of elongation play a key role in understanding of general process of epitaxy and it is important for us to achieve the desired islands and nanowires. However, insight into the island elongation is still limited both in experiment and theory.

With the growth of computing speed, storage density and its application in quantum information, the lithographic methods[17−19] or scanning probe microscopy (SPM) nanofabrication procedures[20,21] have been engaged in semiconductor epitaxy growth for nanostructure. Recently the self-organized island formation has attracted increasing attentions due to its compact and efficient growth procedures[22−28]. Although self-organized island formation has been assessed for the island morphology and formation of island array, much more effort should be paid for the self-organized heteroepitaxy, for example, the research about lateral ordering distribution[24]. Our experiment was performed on the GaAs (100) tilt to (111) 15° at 650 °C and the two-dimensional periodicity was improved with the change of Ga content in GaInP buffer layer. The experimental results demonstrate both InP island morphology and its lateral distribution response to the composition of $Ga_xIn_{1-x}P$ buffer layers.

It is commonly agreed that the energetics of strain relief should play a key role in the growth process[4−7]. The elongation of self-organized islands should associate with the strain energy of islands. In this paper, InP self-organized islands were grown on $Ga_xIn_{1-x}P$ buffer layers with different Ga contents and the remarkable shape elongation modulated by the compositional changes was observed via atomic force microscopy (AFM). To elucidate the mechanism of elongation, we extended an energetic explanation to our experiment firstly. Interestingly, the experiment is consistent with calculation results very much. Thus, the present study elucidated the nanostructrue of islands elongation and its energetic explanation.

A natural qualitative development of facet growth model has been proposed for the elongation of islands. On the other hand, Tersoff *et al.* presented an energetic explanation of the islands elongation. The mismatch between the epitaxial layers and the islands could affect the relax energy as well as the equilibrium shape, while the equilibrium shape of stress coherent epitaxial islands could be achieved by minimizing their total energy with respect to their shape. Therefore, the energetic explanation should provide a powerful tool in studying energetic aspects of elongation of islands.

From Ref. [7], the energetic origin of this elongation can be deduced from the equation: $\frac{E_{\text{total}}}{V} = 2\Gamma(\frac{1}{l}+\frac{1}{w}) - 2ch\left[\frac{1}{l}\ln(\frac{l}{\phi h}) + \frac{1}{w}\ln(\frac{w}{\phi h})\right]$, where $E_{\text{total}} = E_{\text{s}} + E_{\text{r}}$, $\Gamma = \gamma_{\text{e}}\csc\theta - \gamma_{\text{s}}\cot\theta$, $c = \sigma^2(1-\nu)/2\pi u$, and $\phi = \mathrm{e}^{-3/2}\cot\theta$. E_{total} is the total energy of the InP islands, E_{s} is the extra surface energy, and E_{r} is the energy change concerning with the elastic relaxation. V is the volume of the islands. l, w, h, and θ are the length, width, height, and the contact angle of the InP islands, respectively. γ_{e} and γ_{s} are the surface energy of the island's edge facets and the substrate surface energy, respectively. σ is the component of the bulk stress of

1671-7694/2005/0s0012-05 http://www.col.org.cn

the epilayer. ν is the Poisson ratio and u is the shear modulus of the epilayer.

If the E_{total}/V was minimized only with respect to the parameters l and w, $l_{\text{e}} = w_{\text{e}} = \text{e}\phi h \text{e}^{\Gamma/ch}$ is the tradeoff between surface energy and stress, which represents the optimal island metamorphosis. If the contact angle is fixed, it is $l \propto \text{e}^{1/c}$, where c is associated with wetting layer, which means that the buffer layer controls l_{e} — the optimal shape of an island. To our experiment, the c increases with the Ga content in the buffer layer, which means the optimal island shape would become smaller with the mismatch increasing.

All parameters are available from Refs. [41] and [42]. The islands volume is $110^2\times15$ (arbitrary unit), and the height is 15, and the x values are 0.51, 0.7, 0.9 for three samples, respectively. The calculation results are shown in Fig. 1 and the curves 1, 2, 3 represent the samples 1, 2, 3, respectively. When the E/V=−0.6 (a.u.), l/w are 1.11, 1.19, 1.45, respectively. It is clear that the islands elongated as the content of Ga increased in buffer layer with the same E/V.

As for the islands with different volumes, we took the samples with volumes of $100^2\times13$, $110^2\times15$, $120^2\times17$ respectively which have the same Ga content of 0.7. We calculated them to explore the correlation between elongation and buffer contents. The calculation results are shown in Fig. 2, which revealed that the l/w of the islands increased from 1.01, 1.10, to 1.41, elongating with the volume increased at the same energy.

The growth of InP self-organized islands was carried out in a MOCVD system (Veeco, Emcore TurboDisc). The growth diameter is listed in Tables 1 and 2. Here the growth temperature was 650 °C. The growths were carried out on the GaAs substrate (100) tilt to (111) 15°. The substrate was heated to 675 °C and stabilized for 5 minutes to remove the oxidation at the surface, then cooled to 650 °C under the AsH_3 ambient. GaAs buffer layer was grown 10 minutes at the growth rate of 1.6 μm/h with TMGa and AsH_3. GaInP layer was grown on the buffer layers for 4 minutes at the growth rate of 1.7 μm/h with TEGa, TMIn, and PH_3. Controlling the flow ratio of TEGa and TMIn grew the GaInP layers prepared for InP islands. At last the InP was grown for 0.3 minute with TMIn and PH_3. Table 2 gives the detailed reaction parameters. The composition of GaInP listed in Table 2 were measured by X-ray diffraction[33].

Figure 3 shows the represented AFM images of InP self-organized islands of three samples respectively. The characteristic feature of InP on the GaInP is that it stretched along [110] direction and condensed along [1-10] direction. A statistical result to AFM is listed in Table 3.

Take sample 1 for example, the l/w is 1.19 when the diameter of the islands is 467×395 (nm). And the l/w is 1.71 when the mismatch of sample 3 is −6.6%, larger dramatically than sample 1 when the diameter of the islands is 365×213 (nm). It is most likely that the elongation

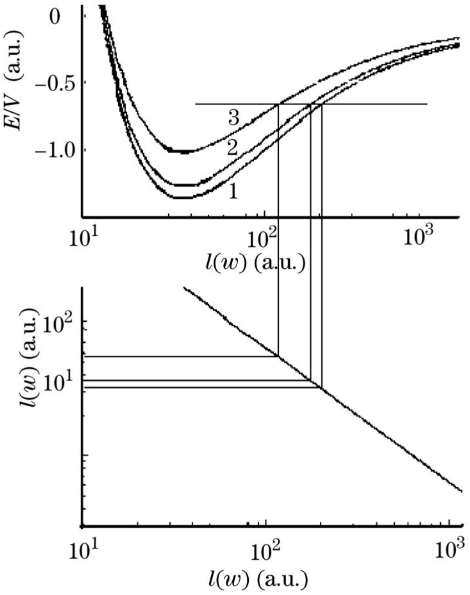

Fig. 1. Energy E/V as a function of l/w *of* island. The island volume is $110^2\times15$ and the height is 15, E/V = −0.6 (a.u.).

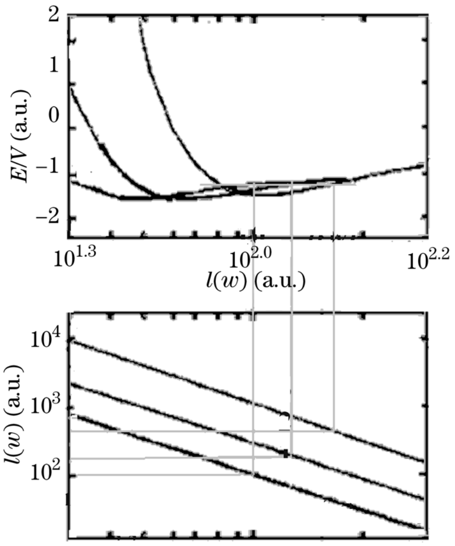

Fig. 2. Formation energy of islands as a function of l/w of islands. Curves 1, 2, 3 represent the islands with the volume of $100^2\times13$, $110^2\times15$, $120^2\times17$ respectively, E/V=−1.0 (a.u.).

Table 1. The Growth Parameters of GaInP Buffer Layers

Sample	GaInP Epilayer		InP Islands	The Composition
	TEGa Flow ($\times10^{-5}$)	TMIn Flow ($\times10^{-5}$)	TMIn Flow ($\times10^{-5}$)	of $\text{Ga}_x\text{In}_{1-x}\text{P}$
1	3.11	2.46	1.64	0.51
2	3.11	1.64	1.64	0.69
3	3.11	0.82	1.64	0.92

Table 2. The Growth Results of InP Islands on GaInP Buffer Layers. Mismatch is Measured by X-rays. The Ratios Are the Roughly Statistical Results

Sample	Lattice Mismatch to InP Islands (%)	D_{110} (nm) (110) Direction	D_{1-10} (nm) (1-10) Direction	D_{110}/D_{1-10}
1	−3.7	335	420	0.79
2	−4.9	291	411	0.71
3	−6.6	206	402	0.51

Table 3. A Statistical Result of the Islands Diameter Transformation Along [110] and [1-10]

Sample	1	2	3
Mismatch Between InP and Wetting Layers (%)	−3.7	−4.9	−6.6
l/w	1.02 (57×56 (nm))	1.06 (56×53 (nm))	1.08 (55×51 (nm))
l/w	1.04 (146×141 (nm))	1.27 (127×99 (nm))	1.34 (134×101 (nm))
l/w	1.19 (467×395 (nm))	1.31 (520×398 (nm))	1.71 (365×213 (nm))

of islands should be highly correlated with the mismatch between the wetting layer and self-organized islands. According to the statistical results, when the content of GaInP is 0.69, the l/w experiences a significant increase from 1.06 (56×53 (nm)) to 1.27 (127×99 (nm)) and to 1.06 (56×53 (nm)) finally, suggesting that the elongation becomes more significant as the volume of the islands increases.

The stress in the self-organized system is very important for the growth of the islands at specific positions because the stress-induced surface could not only dictate the development of a desired morphology, but also affect the nucleation on its surface, including the island nucleation mechanism, nucleation place, the distribution of the island[8−13]. The effective interactions under stress among steps on vicinal surface could form step bunches[14,15], making them to be suitable sites for the nucleation of nanometer-size islands. The corresponding experimental results have been seen in the systems of Ge/Si[34,35], InGaAs/GaAs[36], Si/GaAs[37] etc., and associated lateral distribution of islands were along the step bunch direction[26,38]. The faceted islands (3D island matrix) would appear on the film surface if the step bunches could not enough to release the stress between buffer layer and substrate[26]. The islands mainly formed with {105} facets and distributed regularly on the film surface. This kind of island matrix would be more regular and apparent if the stress-induced superlattice was employed[24,39]. The dislocation would be inevitable when the spontaneous roughness and 3D islands are not enough to release the stress[40,41]. The dislocation regulations of the self-organized island have been reported at Ge/Si, InP/GaInP systems[28,39,42].

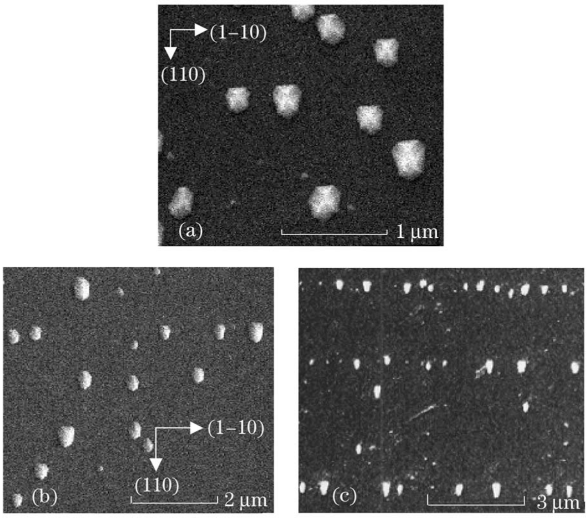

Fig. 3. SEM images of InP/GaInP samples' surface. The numbers are associated with the samples in Table 3.

The island separation distribution abides the scaling theory when the reactants migrate and aggregate at the surface. While the islands nucleate and grow in a large diffusion rates, the island separation distribution n, which gives the probability of finding an island separated by a distance$r$ from another island, is associated with the density of islands N and scaling function[24].

We sorted the islands into different categories in terms of their volume and the formation mechanisms[24]. Figure 4 shows the type-B statistic results. There is no significant difference about the island distribution with the separation r among the 3 samples. Distributed islands of three samples are all abide the distribution function completely or nearly completely. Surprisingly, there are apparent differences existed along [110] and [1-10] directions with Ga content increasing in GaInP buffer layer, as showed in Fig. 5. The islands become more and more orderly averaged along [110] direction with Ga increasing. The fluctuation of island separation distribution along [110] on sample 1 surface is smoother compared with the samples 2 and 3. The distribution of sample 2 fluctuates along [110] direction and reaches the top at 1, 2.69, 4.15, and 5.61 μm respectively, supplying about 1.5-μm periodicity. The sample 3 has only several separated distribution positions: 0.98, 2.69, 4.4, 5.61, and 6.84 μm.

The regular distribution along the [1-10] direction is more significant at sample 3 surface than samples 1 and 2 though the regular distributions also could be found on these two sample surfaces. The sample 1 reaches the top at 1.22, 2.2, 3.17, and 4.02 μm separately with about 0.98-μm distribution. The sample 2 peaks at 0.98,

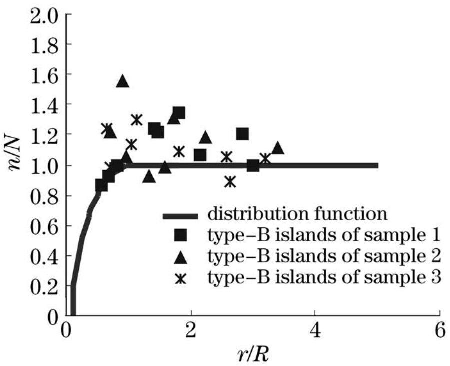

Fig. 4. Scaled radial distribution function for the type-B islands of samples. The solid line is given by $1 - (K(r/M)/K(r_0/M))$, where K is the modified Bessel function of order zero, $M = (1/4\pi N)^{1/2}$, and $r_0 = 0.1R$.

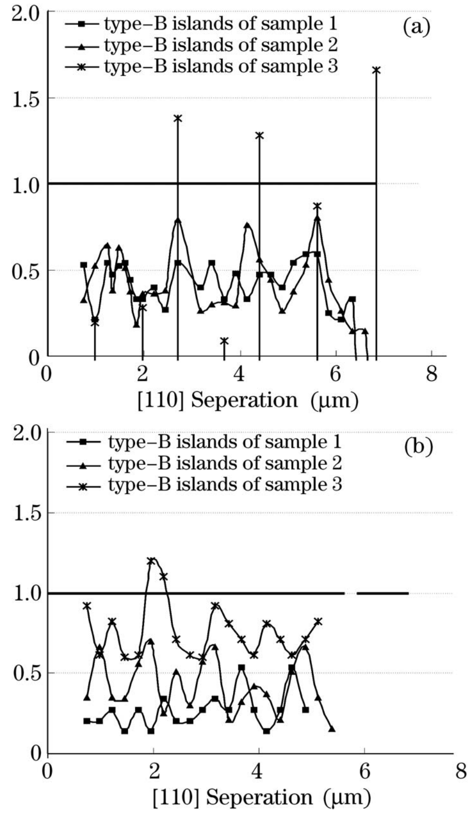

Fig. 5. Separation distribution function along (a) [110] and (b) [1-10] for type-B islands.

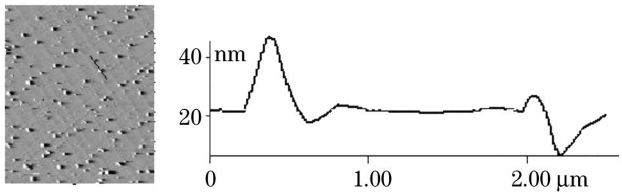

Fig. 6. The AFM result of sample 3 and the height profile through two islands along [110] direction.

1.96, 3.04, and 4.88 μm separately with about 0.96-μm distribution. The sample 3 has top distribution at positions of 1.22, 2.2, 3.17, and 4.15 μm with about 0.98-μm distribution. The periodic distribution along this direction is less apparent compared with the research of Varma *et al.*[24].

The result along [1-10] direction seems consistent with Varma's conclusion that the misoriented substrate could be employed to regulate the self-organized island along [1-10] direction though the mechanism is still not clear. One more result can be obtained that the island distributed periodicity along [1-10] was not much affected by mismatch and dislocation, only the regularity was improved, though it could be affected apparently along [110] direction.

The dislocations appear when the epitaxial layer exceeds the critical thickness, which could be calculated by Matthews and Blakeslee equation[41]. The thicknesses of samples 2 and 3 have exceeded greatly their corresponding critical thicknesses (about 7 and 1.3 nm respectively). The results that samples 2 and 3 have more ordered trend compared with sample 1 which has no mismatch lead to the conclusion that the dislocation plays a key role to regulate self-organized InP island separation distribution on the mismatched buffer layer surface. Figure 6 reveals that the islands are located along the edges of ridge/trough lines. The ridge/trough lines are straight along [1-10] direction, which show a pretty sharp distribution of islands along [110] direction just as the similar result obtained by Shiryaev *et al.* at Ge/Si system[42]. There are many efforts paid to obtain ordered distribution, including the dislocation regulation at Ge/Si system[42,43], $Si_{0.55}Ge_{0.45}$/Si superlattice to Ge quantum dots[44], and the pretreatment to the substrate or mask covering[43,45].

In summary, the elongation of InP self-organized islands could be achieved by the compositional modulation of $Ga_xIn_{1-x}P$ buffer layers successfully. The optimal island volume was found shrinking with increaseing mismatch, and the islands elongated and l/w increased with island volume. With increasing mismatch, the island elongated too. Interestingly, the experimental results could be explained by a Tersoff's theory in our system. This work presented a novel application of energetic explanation for the growth of island elongation. By changing the composition in GaInP buffer layers, it was found the shape and distribution of InP islands on GaInP could be controlled by the stress between GaInP buffer layers and InP islands. The misoriented substrate and the mismatched buffer layer are useful to regulate the two-dimensional ordered self-organized structure. With Ga content increasing in GaInP buffer layers, the island regularity was improved both along [110] and [1-10] directions.

S. Liu's e-mail address is liush@scnu.edu.cn.

References

1. V. M. Kaganer and K. H. Ploog, Phys. Rev. B **64,** 205301 (2001).
2. M. P. Pierre and L. Axel, Physics Today **54,** 46 (2001).
3. S. J. Xu *et al.*, Appl. Phys. Lett. **72,** 3335 (1998).
4. Q. K. K. Liu *et al.*, Phys. Rev. B **60,** 17008 (1999).
5. L. G. Wang *et al.*, Phys. Rev. Lett. **82,** 4042 (1995).
6. J. Platen *et al.*, J. Appl. Phys. **85,** 3957 (1999).
7. J. Tersoff and R. M. Tromp, Phys. Rev. Lett. **70,** 2782 (1993).

8. F. M. Ross, R. M. Tromp, and M. C. Reuter, science **286,** 1931 (1999).
9. Y. W. Mo, D. E. Savage, B. S. Swartzentruber, and M. G. Lagally, Phys. Rev. Lett. **65,** 1020 (1990).
10. N. Richard, T. Jiro, and T. Toshiaki, Nature **369,** 131 (1994).
11. A. Jouni *et al.*, Jpn. J. Appl. Phys. **32,** L35 (1993).
12. D. J. Eaglesham and R. Hull, Mater. Sci. Eng. B **30,** 197 (1995).
13. D. E. Jesson *et al.*, Phys. Rev. Lett. **80,** 5156 (1998).
14. J. B. Hannon, J. Tersoff, and R. M. Tromp, Science **295,** 299 (2002).
15. D. Lacombe *et al.*, Appl. Phys. Lett. **74,** 1680 (1999).
16. Y. W. Zhang, Phys. Rev. B. **61,** 10388(2000).
17. H. R. Eisenberg and D. Kandel, Phys. Rev. B **71,** 115423 (2005).
18. B. Z. Wang *et al.*, Physica E **8,** 290 (2000).
19. J. R. R. Bortoleto, H. R. Gutiérrez, M. A. Cotta, *et al.*, Appl. Phys. Lett. **82,** 3523 (2003).
20. E. R. Glaser, B. R. Bennett, B. V. Shanabrook, *et al.*, Appl. Phys. Lett. **68,** 3614 (1996).
21. H. Pettersson, L. Baath, N. Carlsson, W. Seifert, and L. Samuelson, Appl. Phys. Lett. **79,** 78 (2001).
22. L.-W. Ji, Y. K. Su, S. J. Chang, *et al.*, J. Cryst. Growth **263,** 14 (2004).
23. A. Rastelli, H. Von Känel, B. J. Spencer, and J. Tersoff, Phys. Rev. B **68,** 115301 (2003).
24. S. Varma, C. M. Reaves, V. Bressler-Hill, *et al.*, Surf. Sci. **393,** 24 (1997).
25. F. M. Ross, J. Tersoff, and R. M. Tromp, Phys. Rev. Lett. **80,** 984 (1998).
26. N. Moll, M. Scheffler, and E. Pehlke, Phys. Rev. B **58,** 4566 (1998).
27. F. Q. Liu, Z. G. Wang, B. Xu, *et al.*, Phys. Lett. A **249,** 555 (1998).
28. M. C. Bartelt and J. W. Evans, Phys. Rev. B **46,** 12675 (1992).
29. Bartlett, M. C. Tringides, and J. W. Evans, Phys. Rev. B **47,** 13891 (1993).
30. H. Wang, C. Liao, *et al.*, J. South China Normal University **100,** 56 (2003).
31. H. Wang, C. Liao, *et al.*, College Physics **20,** 30 (2001).
32. W. A. Brantley, J. Appl. Phys. **44,** 534 (1973).
33. E. F. Steigmeier, Appl. Phys. Lett. **3,** 6 (1956).
34. H. Wang *et al.*, J. Synthetic Cryst. **33,** 549 (2004).
35. H. Wang *et al.*, J. Synthetic Cryst. **33,** 96 (2004).
36. M. Hammar, F. K. LeGoues, J. Tersoff, M. C. Reuter, and R. M. Tromp, Surf. Sci. **349,** 129 (1996).
37. J. B. Hannon, F. J. Meyer zu Heringdorf, J. Tersoff, and R. M.Tromp, Phys. Rev. Lett. **86,** 4871 (2001).
38. J. A. Floro, G. A. Lucadamo, E. Chason, *et al.*, Phys. Rev. Lett. **80,** 4717 (1998).
39. L. Wang and A. Zunger, J. Phys. Chem. **98,** 2158 (1994).
40. K. Matsuda, T. Saiki, S. Nomura, *et al.*, Phys. Rev. Lett. **91,** 177401 (2003).
41. K. R. Elder, M. Katakowski, M. Haataja, *et al.*, Phys. Rev. Lett. **88,** 245701 (2002).
42. S. Y. Shiryaev, F. Jensen, J. L. Hansen, *et al.*, Phys. Rev. Lett. **78,** 503 (1997).
43. C. Teichert, Physics Reports **365,** 335 (2002).
44. J. Zhu, K. Brunner, and G. Abstreiter, Appl. Phys. Lett. **73,** 620 (1998).
45. H. Lee, J. A. Johnson, M. Y. He, J. S. Speck, and P. M. Petroffa, Appl. Phys. Lett. **78,** 105 (2001).